QUANTIFICATION OF SEISMIC ENERGY DEMAND IN NONLINEAR STRUCTURES THROUGH ANALYTICAL DERIVATIONS

S.L. McCabe[(1)], K.K.F. Wong[(2)]

[(1)] *Director, National Earthquake Hazards Reduction Program, USA, smccabe@nist.gov*
[(2)] *Research Structural Engineer, National Institute of Standards and Technology, USA, kfwong@nist.gov*

Abstract

The classical seismic design procedure uses a force-based approach where reduced seismic force demands are evaluated and compared to the corresponding seismic capacities. An improved performance-based design procedure recently developed uses the displacement-based approach to ensure that structures with nonlinear deformations perform within acceptable limits. However, neither of these procedures considers the effect of cyclic behavior that is typically observed in the seismic response of nonlinear structures.

On the other hand, energy is the product of force and displacement, which captures both monotonic and cyclic behavior of structural response. At the same time, structures suffering damage from a major earthquake participate in an energy transfer process. Earthquake ground motion transfers energy to individual structures as input energy that induces vibrations in the structure and its contents, resulting in response in terms of potential energy, kinetic energy, and damping energy. Quantifying these energy demands is often difficult, particularly in the calculation of potential energy, where earthquake often causes both material and geometric nonlinearities in the structure. Since the potential energy relates to the stiffness of the structure, it consists of three parts: (1) Strain energy associated with the elastic portion of the material; (2) Higher-order energy associated with geometric nonlinearity of the structure; and (3) Plastic energy associated with material nonlinearity of the structural components.

In this research, an analytical derivation is used to quantify the energy demand in fully nonlinear framed structures using an energy balance approach. A moment-resisting steel frame is used to verify the method by evaluating the energy response and the transfer among different energy forms throughout the dynamic analysis. The result shows that plastic energy dissipated at each plastic hinge is a positive, scalar quantity that can be calculated uniquely, and the sum of individual plastic energy at each plastic hinge is exactly equal to the overall plastic energy of the structure. Once energy demand is quantified uniquely, structural performance and damage can be assessed more easily via comparison of the energy demand with the corresponding energy capacity. Through this process of quantifying the seismic performance of structures, higher level of confidence can be achieved in the design over the current force-based or displacement-based methods.

Keywords: Energy demand; Energy capacity; Plastic energy; Material nonlinearity; Geometric nonlinearity

1. Introduction

Current seismic design procedures use either a force-based or displacement-based approach to ensure that structures can perform adequately during major events. However, neither of these procedures considers the effect of cyclic behavior that is typically observed in the seismic response of nonlinear structures. Accumulation of damage as a function of the number of inelastic cycles has been recognized in laboratory as well as post-earthquake reconnaissance. The question often raised is how to relate maximum responses with some measure of damage. Recognizing this shortcoming in the current procedure, energy, as a product of force and displacement, can capture both monotonic and cyclic behavior. Therefore, a study on how energy can be used in structural design is worthwhile, particularly how energy demand and capacity are quantified.

Research on seismic energy began in the 1980s when it was recognized that significant cumulative damage can occur in structures without large global displacement responses in long-duration earthquake ground motions [1-4]. However, these studies focused on evaluating the hysteretic energy by calculating the enclosed area in a force-deformation curve of single degree of freedom systems. In 1990, an analytical procedure was developed to clearly define different forms of energy for linear multi-degree of freedom structures [5], and this procedure is later extended in 2002 to define energy due to inelastic deformation [6]. However, these studies did not consider the reduction of lateral stiffness by axial load due to geometric nonlinearity, which can lead to considerable error in the energy calculations.

In this research, an analytical method for calculating energy considering both geometric and material nonlinearities is derived to investigate the energy of framed structures responding nonlinearly to earthquakes. In particular, the potential energy that is directly related to nonlinear stiffness of the structure is investigated, and a step-by-step analysis of a one-story frame is used to verify that input energy is balanced by potential energy throughout the static loading and unloading phases. This potential energy consists of three parts in a fully nonlinear system: (1) the stored linear elastic "strain energy"; (2) the "higher-order energy" associated with geometric nonlinearity; and (3) the "plastic energy" dissipated by material nonlinearity. Finally, four-story frame is used to verify energy balance can also be achieved in a dynamic context.

2. Inelastic Displacement for Material Nonlinearity

The derivation on the use of inelastic displacement for analyzing structures with material nonlinearity has previously been published [6-7] and is briefly summarized here with an extension to include geometric nonlinearity. Consider a framed structure having a total of *n* degrees of freedom (DOFs) and *m* plastic hinge locations (PHLs). Let the $n\times 1$ total displacement $\mathbf{x}(t)$ at each DOF be represented as the summation of the $n\times 1$ elastic displacement $\mathbf{x}'(t)$ and the $n\times 1$ inelastic displacement $\mathbf{x}''(t)$:

$$\mathbf{x}(t)=\mathbf{x}'(t)+\mathbf{x}''(t) \tag{1}$$

Similarly, let the $m\times 1$ total moment $\mathbf{m}(t)$ at the PHLs of a moment-resisting frame be separated into the $m\times 1$ elastic moment $\mathbf{m}'(t)$ and the $m\times 1$ inelastic moment $\mathbf{m}''(t)$:

$$\mathbf{m}(t)=\mathbf{m}'(t)+\mathbf{m}''(t) \tag{2}$$

This inelastic moment $\mathbf{m}''(t)$ is often known as the "residual moment" that is caused by material nonlinearity in the structure. The displacements in Eq. (1) and the moments in Eq. (2) are related by the equations:

$$\mathbf{m}'(t)=\mathbf{K}'(t)^T\mathbf{x}'(t) \quad , \quad \mathbf{m}''(t)=-\left[\mathbf{K}''(t)-\mathbf{K}'(t)^T\mathbf{K}(t)^{-1}\mathbf{K}'(t)\right]\mathbf{\Theta}''(t) \tag{3}$$

where $\mathbf{\Theta}''(t)$ is the $m\times 1$ plastic rotation at each PHL, and $\mathbf{K}(t)$, $\mathbf{K}'(t)$, and $\mathbf{K}''(t)$ are time-varying stiffness matrices due to geometric nonlinearity in which columns are subjected to time-varying axial compressive forces $P(t)$. Since the total axial force in all columns within a single floor remains constant, software developers generally assume that all stiffness matrices remain constant throughout the duration of the earthquakes to simplify the calculations without losing accuracy. Doing so, Eq. (3) becomes

$$\mathbf{m}'(t) = \mathbf{K}'^T \mathbf{x}'(t) \quad , \quad \mathbf{m}''(t) = -\left[\mathbf{K}'' - \mathbf{K}'^T \mathbf{K}^{-1} \mathbf{K}'\right] \mathbf{\Theta}''(t) \tag{4}$$

The relationship between the plastic rotation $\mathbf{\Theta}''(t)$ and inelastic displacement $\mathbf{x}''(t)$ can be written as

$$\mathbf{x}''(t) = \mathbf{K}^{-1} \mathbf{K}' \mathbf{\Theta}''(t) \tag{5}$$

Substituting both equations in Eq. (4) into Eq. (2) and then making use of Eqs. (1) and (5) gives the governing equation for calculating the plastic hinge responses for any total displacement pattern $\mathbf{x}(t)$:

$$\mathbf{m}(t) + \mathbf{K}'' \mathbf{\Theta}''(t) = \mathbf{K}'^T \mathbf{x}(t) \tag{6}$$

3. Dynamic Equilibrium Equation of Motion

For a moment-resisting framed structure modeled as an n DOF system and subjected to earthquake ground motions, the dynamic equilibrium equation of motion can be written as

$$\mathbf{M}\ddot{\mathbf{x}}(t) + \mathbf{C}\dot{\mathbf{x}}(t) + \mathbf{K}\mathbf{x}'(t) = -\mathbf{M}\ddot{\mathbf{g}}(t) - \mathbf{F}_a(t) \tag{7}$$

where $\mathbf{M}$ is the $n \times n$ mass matrix, $\mathbf{C}$ is the $n \times n$ damping matrix, $\dot{\mathbf{x}}(t)$ is the $n \times 1$ velocity vector, $\ddot{\mathbf{x}}(t)$ is the $n \times 1$ acceleration vector, $\mathbf{K}$ is the same $n \times n$ stiffness matrix presented in Eq. (4), $\ddot{\mathbf{g}}(t)$ is the $n \times 1$ earthquake ground acceleration vector corresponding to the effect of ground motion at each DOF, and $\mathbf{F}_a(t)$ is the $n \times 1$ vector of additional forces imposed on the structure due to geometric nonlinearity accounting for all the gravity columns in the structure (mainly the P-Δ effect). In a two-dimensional analysis, the relationship between this lateral force $\mathbf{F}_a(t)$ and the lateral displacement $\mathbf{x}(t)$ can be written as

$$\mathbf{F}_a(t) = \mathbf{K}_a \mathbf{x}(t) \tag{8}$$

where $\mathbf{K}_a$ is an $n \times n$ stiffness matrix that is a function of the gravity loads on the leaning column and the corresponding story height, which can be written in the form:

$$\mathbf{K}_a = \begin{bmatrix} -Q_1/h_1 - Q_2/h_2 & Q_2/h_2 & 0 & \cdots & 0 \\ Q_2/h_2 & -Q_2/h_2 - Q_3/h_3 & \ddots & \ddots & \vdots \\ 0 & \ddots & \ddots & Q_{n-1}/h_{n-1} & 0 \\ \vdots & \ddots & Q_{n-1}/h_{n-1} & -Q_{n-1}/h_{n-1} - Q_n/h_n & Q_n/h_n \\ 0 & \cdots & 0 & Q_n/h_n & -Q_n/h_n \end{bmatrix} \tag{9}$$

Here, Q_i is the total axial force due to gravity loads acting on the leaning column of the ith floor, and h_i is the story height of the ith floor. Now substituting Eq. (8) into Eq. (7) and rearranging terms gives

$$\mathbf{M}\ddot{\mathbf{x}}(t) + \mathbf{C}\dot{\mathbf{x}}(t) + \mathbf{K}\mathbf{x}'(t) + \mathbf{K}_a \mathbf{x}(t) = -\mathbf{M}\ddot{\mathbf{g}}(t) \tag{10}$$

Since $\ddot{\mathbf{y}}(t) = \ddot{\mathbf{x}}(t) + \ddot{\mathbf{g}}(t)$ where $\ddot{\mathbf{y}}(t)$ is the $n \times 1$ absolute acceleration vector, substituting this equation into Eq. (10) gives the governing equation of motion for energy balance:

$$\mathbf{M}\ddot{\mathbf{y}}(t) + \mathbf{C}\dot{\mathbf{x}}(t) + \mathbf{K}\mathbf{x}'(t) + \mathbf{K}_a \mathbf{x}(t) = \mathbf{0} \tag{11}$$

4. Energy Balance

To evaluate seismic energy, integrating Eq. (11) over the path of displacement response gives

$$\int_0^t \ddot{\mathbf{y}}(t)^T \mathbf{M} d\mathbf{x} + \int_0^t \dot{\mathbf{x}}(t)^T \mathbf{C} d\mathbf{x} + \int_0^t \mathbf{x}'(t)^T \mathbf{K} d\mathbf{x} + \int_0^t \mathbf{x}(t)^T \mathbf{K}_a d\mathbf{x} = 0 \tag{12}$$

Note that $d\mathbf{x}(t) = d\mathbf{y}(t) - d\mathbf{g}(t)$, where $\mathbf{y}(t)$ is the $n \times 1$ absolute displacement vector and $\mathbf{g}(t)$ is the $n \times 1$ earthquake ground displacement vector. Substituting this equation into the first integral of Eq. (12) gives

$$\int_0^t \ddot{\mathbf{y}}(t)^T \mathbf{M} d\mathbf{y} + \int_0^t \dot{\mathbf{x}}(t)^T \mathbf{C} d\mathbf{x} + \int_0^t \mathbf{x}'(t)^T \mathbf{K} d\mathbf{x} + \int_0^t \mathbf{x}(t)^T \mathbf{K}_a d\mathbf{x} = \int_0^t \ddot{\mathbf{y}}(t)^T \mathbf{M} d\mathbf{g} \tag{13}$$

In addition, the incremental displacement $d\mathbf{x}(t)$ can be separated into elastic displacement and inelastic displacement as $d\mathbf{x}(t) = d\mathbf{x}'(t) + d\mathbf{x}''(t)$. Substituting this equation into the third integral of Eq. (13) gives

$$\int_0^t \ddot{\mathbf{y}}(t)^T \mathbf{M} d\mathbf{y} + \int_0^t \dot{\mathbf{x}}(t)^T \mathbf{C} d\mathbf{x} + \int_0^t \mathbf{x}'(t)^T \mathbf{K} d\mathbf{x}' + \int_0^t \mathbf{x}'(t)^T \mathbf{K} d\mathbf{x}'' + \int_0^t \mathbf{x}(t)^T \mathbf{K}_a d\mathbf{x} = \int_0^t \ddot{\mathbf{y}}(t)^T \mathbf{M} d\mathbf{g} \tag{14}$$

Each integral in Eq. (14) is considered separately in the following sub-sections.

4.1 Kinetic Energy (*KE*)

The first integral on the left-hand side of Eq. (14) represents the absolute kinetic energy (*KE*) and can be evaluated using the absolute velocity of the structure as:

$$KE(t_k) = \int_0^{t_k} \ddot{\mathbf{y}}(t)^T \mathbf{M} d\mathbf{y} = \frac{1}{2}\dot{\mathbf{y}}(t_k)^T \mathbf{M}\dot{\mathbf{y}}(t_k) - \frac{1}{2}\dot{\mathbf{y}}(0)^T \mathbf{M}\dot{\mathbf{y}}(0) = \frac{1}{2}\dot{\mathbf{y}}_k^T \mathbf{M}\dot{\mathbf{y}}_k \tag{15}$$

where $\dot{\mathbf{y}}(t)$ is the $n \times 1$ absolute velocity vector, $\dot{\mathbf{y}}_k$ represents the discretized form of $\dot{\mathbf{y}}(t_k)$, and t_k represents the kth time step at which the energy value is calculated. The structure is assumed to be at rest when the earthquake begins, and therefore $\dot{\mathbf{y}}(0) = \mathbf{0}$. Due to the squaring of the absolute velocity vector in Eq. (15) and a positive definite **M** matrix, the kinetic energy is always positive.

4.2 Damping Energy (*DE*)

The second integral on the left-hand side of Eq. (14) represents the damping energy (*DE*), which is the energy dissipated via viscous damping mechanism within the structure. The integrand is always positive, and therefore damping energy always accumulates over time. In terms of numerical simulation, the integral can be numerically approximated by evaluating the area underneath the curve using the trapezoidal rule:

$$DE(t_k) = \int_0^{t_k} \dot{\mathbf{x}}(t)^T \mathbf{C} d\mathbf{x} = \sum_{k=1}^{t_k} \frac{1}{2}\left(\dot{\mathbf{x}}_{k-1}^T + \dot{\mathbf{x}}_k^T\right) \mathbf{C} \left(\mathbf{x}_k - \mathbf{x}_{k-1}\right) \tag{16}$$

where $\mathbf{x}_k$ represents the discretized form of $\mathbf{x}(t_k)$ and $\dot{\mathbf{x}}_k$ represents the discretized forms of $\dot{\mathbf{x}}(t_k)$.

4.3 Strain Energy (*SE*)

The third integral on the left-hand side of Eq. (14) represents the strain energy (*SE*) of the moment-resisting frame and can be evaluated as:

$$SE(t_k) = \int_0^{t_k} \mathbf{x}'(t)^T \mathbf{K} d\mathbf{x}' = \frac{1}{2}\mathbf{x}'(t_k)^T \mathbf{K}\mathbf{x}'(t_k) - \frac{1}{2}\mathbf{x}'(0)^T \mathbf{K}\mathbf{x}'(0) = \frac{1}{2}\mathbf{x}_k'^T \mathbf{K}\mathbf{x}_k' \tag{17}$$

where $\mathbf{x}_k'$ represents the discretized form of $\mathbf{x}'(t_k)$. The structure is again assumed to be at rest when the earthquake begins, and therefore $\mathbf{x}'(0) = \mathbf{0}$. Due to the squaring of the elastic displacement vector in Eq. (17) and a positive definite **K** matrix, the strain energy is always positive.

4.4 Plastic Energy (*PE*)

The fourth integral on the left-hand side of Eq. (14), which is associated with inelastic displacements, represents the plastic energy (*PE*) dissipated by the permanent deformations of the structure. Rewriting Eqs. (4) and (5) in the forms:

$$\mathbf{K} d\mathbf{x}'' = \mathbf{K}' d\mathbf{\Theta}'' \quad , \quad \mathbf{x}'(t)^T \mathbf{K}' = \mathbf{m}'(t)^T \tag{18}$$

Then substituting Eq. (18) into the fifth integral of Eq. (14) gives

$$PE(t_k) = \int_0^{t_k} \mathbf{x}'(t)^T \mathbf{K} d\mathbf{x}'' = \int_0^{t_k} \mathbf{x}'(t)^T \mathbf{K}' d\mathbf{\Theta}'' = \int_0^{t_k} \mathbf{m}'(t)^T d\mathbf{\Theta}'' = \sum_{i=1}^{m} \int_0^{t_k} m_i'(t) d\theta_i'' = \sum_{i=1}^{m} PE_i(t_k) \tag{19}$$

where PE_i represents the plastic energy dissipation at the ith plastic hinge, $i = 1,...,m$. Through this analytical derivation, it is proven in Eq. (19) that the overall plastic energy dissipation $PE(t_k)$ is exactly equal to the sum of plastic energy dissipation in all the plastic hinges $PE_i(t_k)$.

The term PE_i in Eq. (19) can be numerically approximated by evaluating the area underneath the curve using the trapezoidal rule:

$$PE_i = \int_0^{t_k} m_i'(t) d\theta_i'' = \sum_{k=1}^{t_k} \frac{1}{2}\left(m_{i,k-1}' + m_{i,k}'\right)\left(\theta_{i,k}'' - \theta_{i,k-1}''\right) \tag{20}$$

where $m_{i,k}'$ and $\theta_{i,k}''$ represent the discretized forms of $m_i'(t_k)$ and $\theta_i''(t_k)$, respectively. Note that PE_i is computed by integrating the product of elastic moment m_i' and the change in plastic rotation $d\theta_i''$. A positive change in plastic rotation is always caused by a positive moment, and a negative change in plastic rotation is always caused by a negative moment. Therefore, PE_i is always positive and accumulates over time.

4.5 Higher-order Energy (*HE*)

The fifth integral on the left-hand side of Eq. (14) represents higher-order energy (*HE*) due to gravity loads on the structure itself. It is of higher-order because the energy comes from the large *P*-Δ effect, where gravity in the vertical direction is producing energy while going through movement in the horizontal direction. This energy is calculated as follows:

$$HE(t_k) = \int_0^{t_k} \mathbf{x}(t)^T \mathbf{K}_a d\mathbf{x} = \frac{1}{2}\mathbf{x}(t_k)^T \mathbf{K}_a \mathbf{x}(t_k) - \frac{1}{2}\mathbf{x}(0)^T \mathbf{K}_a \mathbf{x}(0) = \frac{1}{2}\mathbf{x}_k^T \mathbf{K}_a \mathbf{x}_k \tag{21}$$

where the structure is again assumed to be at rest when the earthquake begins, and therefore $\mathbf{x}(0) = \mathbf{0}$. Due to the squaring of the total displacement vector in Eq. (21) and a negative definite $\mathbf{K}_a$ matrix as presented in Eq. (9), the higher-order energy is always negative and varies with time.

4.6 Input Energy (*IE*)

Finally, the integral on the right-hand side of Eq. (14) represents the absolute input energy (*IE*) due to the earthquake ground motion, and this integral can be numerically approximated by evaluating the area underneath the ground motion curve using the trapezoidal rule:

$$IE(t_k) = \int_0^{t_k} \ddot{\mathbf{y}}(t)^T \mathbf{M} d\mathbf{g} = \sum_{k=1}^{t_k} \frac{1}{2}\left(\ddot{\mathbf{y}}_{k-1}^T + \ddot{\mathbf{y}}_k^T\right)\mathbf{M}\left(\mathbf{g}_k - \mathbf{g}_{k-1}\right) \tag{22}$$

where $\ddot{\mathbf{y}}_k$ represents the discretized form of $\ddot{\mathbf{y}}(t_k)$ and $\mathbf{g}_k$ represents the discretized form of $\mathbf{g}(t_k)$.

In summary, substituting Eqs. (15), (16), (17), (19), (21), and (22) into Eq. (14), the energy balance equation becomes

$$KE + DE + SE + HE + PE = IE \tag{23}$$

5. Energy Balance Verification

To verify the energy is balanced in Eq. (23), consider a one-story one-bay frame as shown in Fig.1a. Assume an elastic modulus of $E = 200$ GPa and a moment of inertia of $I = 4.16 \times 10^8$ mm^4 for both the beam and columns. Also let the gravity load be $P = 5340$ kN acting on each column, which is equivalent to 13.6 % of the critical buckling load (i.e., $P/P_{cr} = 0.136$). Finally, six plastic hinges are included in the model as shown in Fig.1a with labels from #1 to #6. Assume material exhibits elastic-perfectly-plastic behavior with moment capacities $m_c = 3909$ kN·m for the columns and $m_b = 3130$ kN·m for the beam.

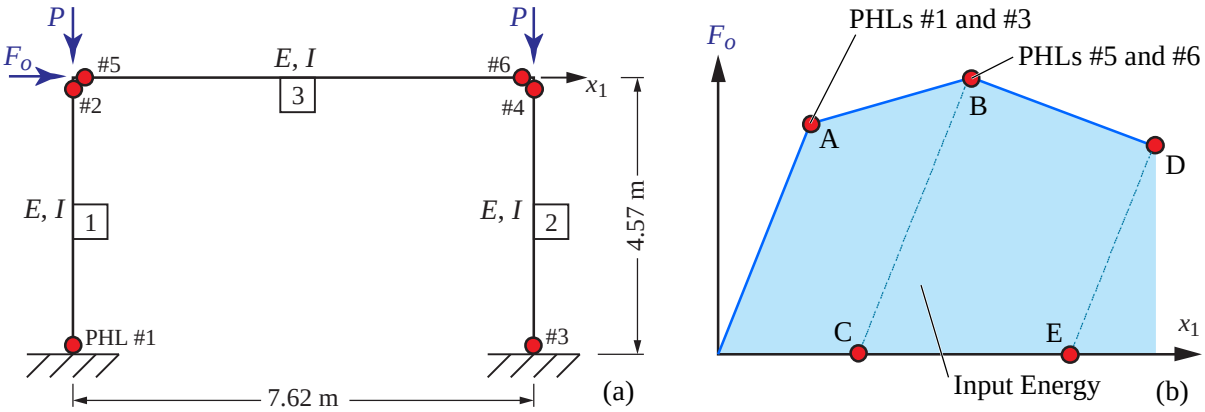

Fig. 1 – One-story one-bay moment resisting frame

No leaning column is used in the model, and therefore $HE = 0$. Now consider a static horizontal load F_o is incrementally applied to the frame. A typical pushover curve for the frame is shown in Fig.1b, where Point A shows the yielding of PHLs #1 and #3, and Point B shows the yielding of PHLs #5 and #6. Input energy (*IE*) is calculated by determining the area underneath the curve as highlighted in blue. With static load being applied, $KE = DE = 0$. Therefore, the energy balance equation in Eq. (23) becomes

$$SE + PE = IE \tag{24}$$

5.1 Loading Up to Point A

First consider Point A shown in Fig.1b, where the moments in PHLs #1 and #3 are exactly equal to the maximum moment capacities. At this point, the applied force is $F_o = 2289$ kN, and the resulting displacement is $x_1 = 0.229$ m as shown in Fig.2a. This gives an elastic stiffness of the frame of $K = F_o / x_1 = 9996$ kN/m. The resultant forces of each member are shown in Fig.2b, and Fig.2c shows that PHLs #1 and #3 are at yield, while PHLs #5 and #6 are below yield. The energy quantities are calculated as:

$$SE = \frac{1}{2}(9996)(0.229)^2 = 262 \text{ kJ} \quad , \quad PE = 0 \text{ kJ} \quad , \quad IE = \frac{1}{2}(0.229)(2289) = 262 \text{ kJ} \tag{25}$$

Therefore, from Eq. (25), $SE + PE = IE$, and Eq. (24) is satisfied.

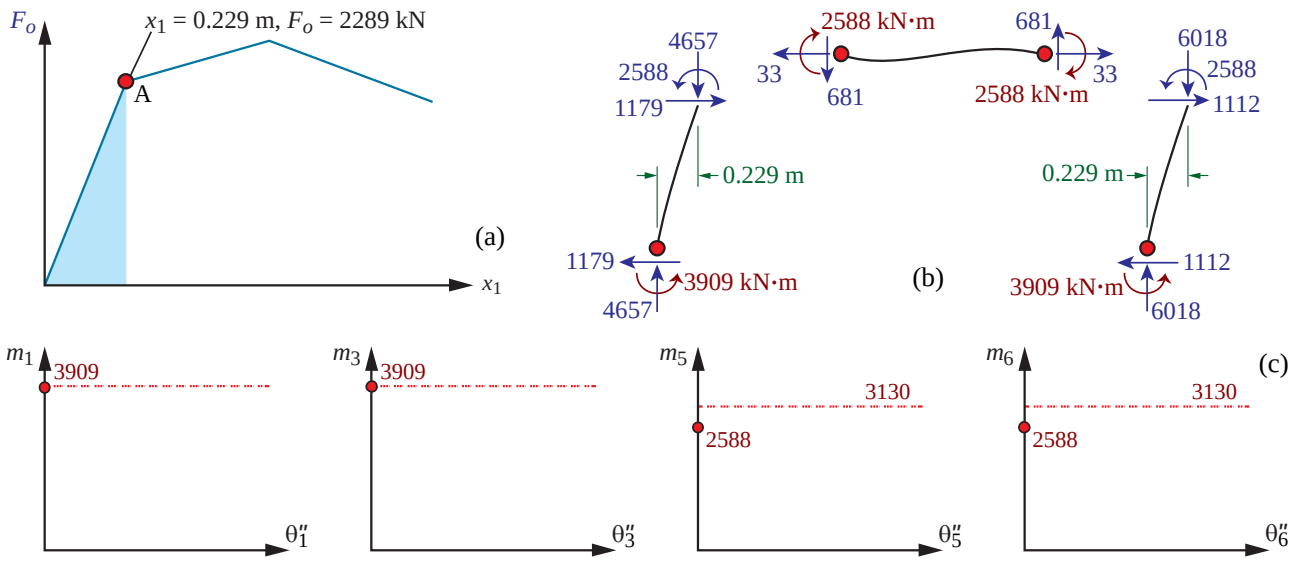

Fig. 2 – State of structure at Point A

5.2 Loading Up to Point B

Now let the applied force be increased up to Point B shown in Fig.1b, where the moments in PHLs #5 and #6 are exactly equal to the moment capacities. At this point, the applied force is $F_o = 2326$ kN, and the resulting displacement is $x_1 = 0.316$ m as shown in Fig.3a. The resultant forces of each member are shown in Fig.3b, and Fig.3c shows that PHLs #5 and #6 are at yield, while PHLs #1 and #3 are beyond yield with plastic rotations of $\theta_1'' = \theta_3'' = 0.0245$ rad. Note that the moments m_1 and m_3 are below the moment capacity of the columns due to axial force and yield moment interactions. Corresponding to the plastic rotations in PHLs #1 and #3, the elastic moments are calculated to be $m_1' = 3923$ kN·m and $m_3' = 2924$ kN·m, and therefore the inelastic moments are $m_1'' = -40$ kN·m and $m_3'' = -62$ kN·m. The energy quantities are calculated as:

$$PE_1 = \frac{3883+3923}{2}(0.0245) = 96 \text{ kJ} \quad , \quad PE_3 = \frac{3862+3924}{2}(0.0245) = 95 \text{ kJ} \tag{26a}$$

$$SE = \frac{1}{2}\frac{(2326)^2}{9996} = 271 \text{ kJ} \quad , \quad IE = 262 + \frac{(2326+2289)}{2}(0.316-0.229) = 462 \text{ kJ} \tag{26b}$$

$$PE = PE_1 + PE_3 = 191 \text{ kJ} \tag{26c}$$

Therefore, from Eqs. (26b) and (26c), $SE + PE = IE$, and Eq. (24) is satisfied.

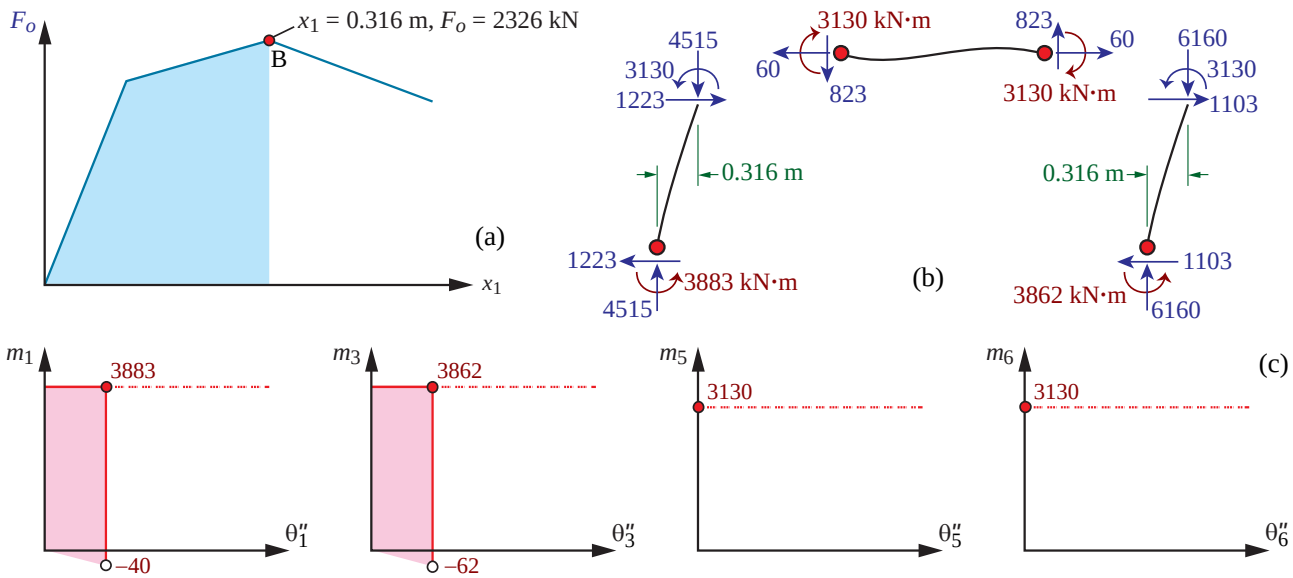

Fig. 3 – State of structure at Point B

5.3 Unloading to Point C

Now let the applied force be completely removed to reach Point C shown in Fig.1b. At this point, the applied force is $F_o = 0$ kN, and the resulting displacement is $x_1 = x_1'' = 0.084$ m (i.e., the elastic displacement $x_1' = 0$) as shown in Fig.4a. The resultant forces of each member are shown in Fig.4b, and Fig.4c shows that PHLs #5 and #6 are elastic, while PHLs #1 and #3 unload to negative moments of $m_1 = m_1'' = -40$ kN·m and $m_3 = m_3'' = -62$ kN·m (i.e., the elastic moments $m_1' = m_3' = -40$). Since plastic energy remains the same during unloading, i.e., $PE_1 = 96$ kJ and $PE_3 = 95$ kJ, the energy quantities are calculated as:

$$SE = 0 \text{ kJ} \quad , \quad PE = PE_1 + PE_3 = 191 \text{ kJ} \quad , \quad IE = 462 - \frac{1}{2}\frac{(2326)^2}{9996} = 191 \text{ kJ} \tag{27}$$

Therefore, from Eq. (27), $SE + PE = IE$, and Eq. (24) is satisfied.

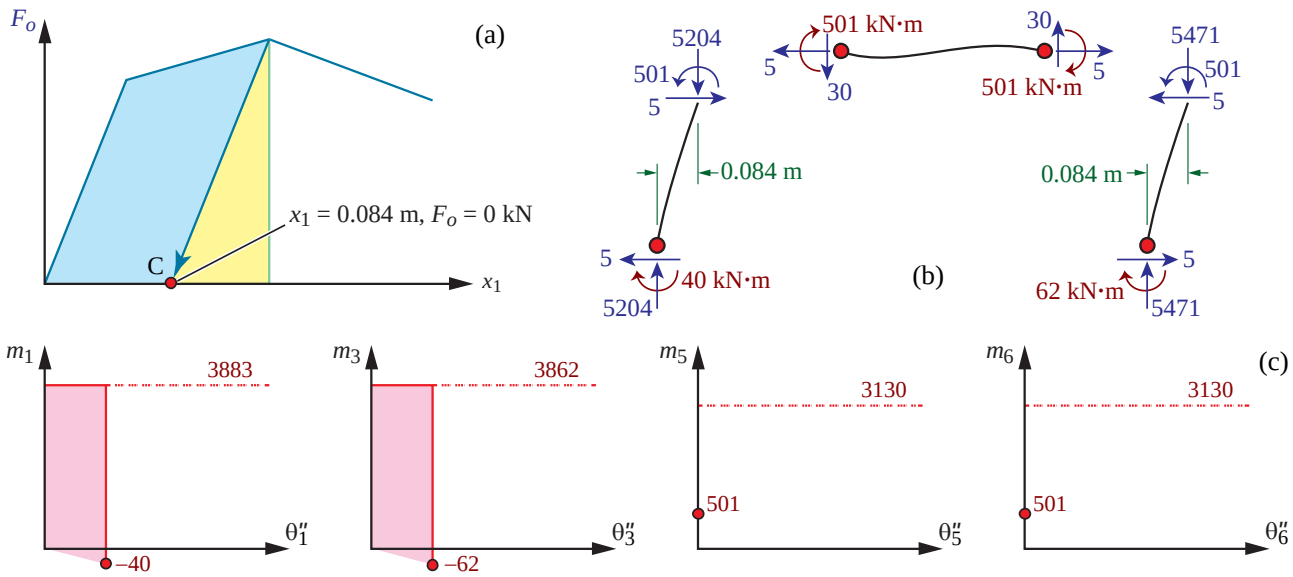

Fig. 4 – State of structure at Point C

5.4 Reloading Up to Point D

Now let the applied force resumes and continues beyond Point B until reaching Point D shown in Fig.1b. At this point, a yield mechanism has formed, which means any additional load can cause instability of the frame. For this reason, displacement control is used. Let the displacement of the frame be $x_1 = 0.457$ m, and the corresponding applied force is calculated to be $F_o = 1995$ kN as shown in Fig.5a. The resultant forces of each member are shown in Fig.5b, and Fig.5c shows that PHLs #1, #3, #5, and #6 are beyond yield with plastic rotations of $\theta_1'' = \theta_3'' = 0.0556$ rad and $\theta_5'' = \theta_6'' = 0.0309$ rad. Corresponding to these plastic rotations, the inelastic moments are shown in Fig.5c. The energy quantities are then calculated as:

$$PE_1 = 96 + (3883 + 40 + 3883 - 515)(0.0556 - 0.0245)/2 = 209 \text{ kJ} \tag{28a}$$

$$PE_3 = 95 + (3862 + 62 + 3862 - 493)(0.0556 - 0.0245)/2 = 208 \text{ kJ} \tag{28b}$$

$$PE_5 = PE_6 = (3130 - 501 + 3130 - 873)(0.0309)/2 = 75.5 \text{ kJ} \tag{28c}$$

$$PE = PE_1 + PE_3 + PE_5 + PE_6 = 568 \text{ kJ} \tag{28d}$$

$$SE = \frac{1}{2}\frac{(1995)^2}{9996} = 199 \text{ kJ} \quad , \quad IE = 462 + \frac{1}{2}(1995 + 2326)(0.457 - 0.316) = 767 \text{ kJ} \tag{28e}$$

Therefore, from Eqs. (28d) and (28e), $SE + PE = IE$, and Eq. (24) is satisfied.

5.5 Unloading to Point E

Finally, let the applied force be completely removed to reach Point E shown in Fig.1b. At this point, the applied force is $F_o = 0$ kN, and the resulting displacement is $x_1 = x_1'' = 0.258$ m as shown in Fig.5a. The resultant forces of each member are shown in Fig.5b, and Fig.5c shows the moment-rotation plot of each plastic hinge. Since the strain energy at zero force is $SE = 0$ kJ, and the plastic energy remains the same during unloading, i.e., $PE_1 = 209$ kJ, $PE_3 = 208$ kJ, and $PE_5 = PE_6 = 75.5$ kJ, the energy quantities are calculated as:

$$SE = 0 \text{ kJ} \quad , \quad PE = PE_1 + PE_3 + PE_5 + PE_6 = 568 \text{ kJ} \quad , \quad IE = 767 - \frac{1}{2}\frac{(1995)^2}{9996} = 568 \text{ kJ} \tag{29}$$

Therefore, from Eq. (29), $SE + PE = IE$, and Eq. (24) is satisfied.

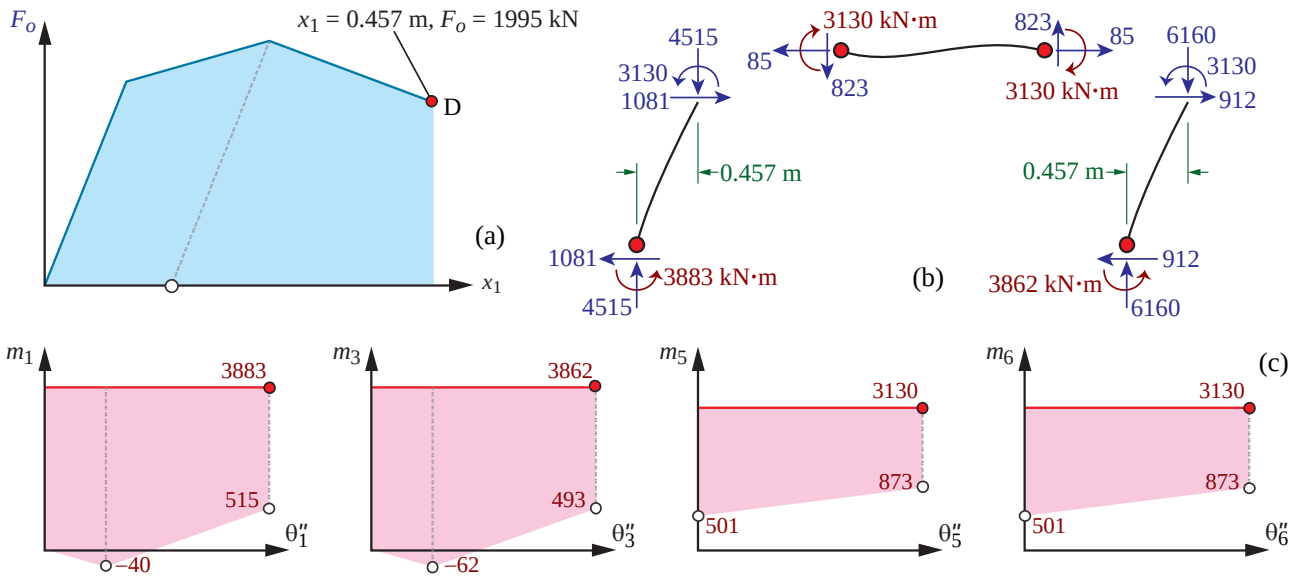

Fig. 5 – State of structure at Point D

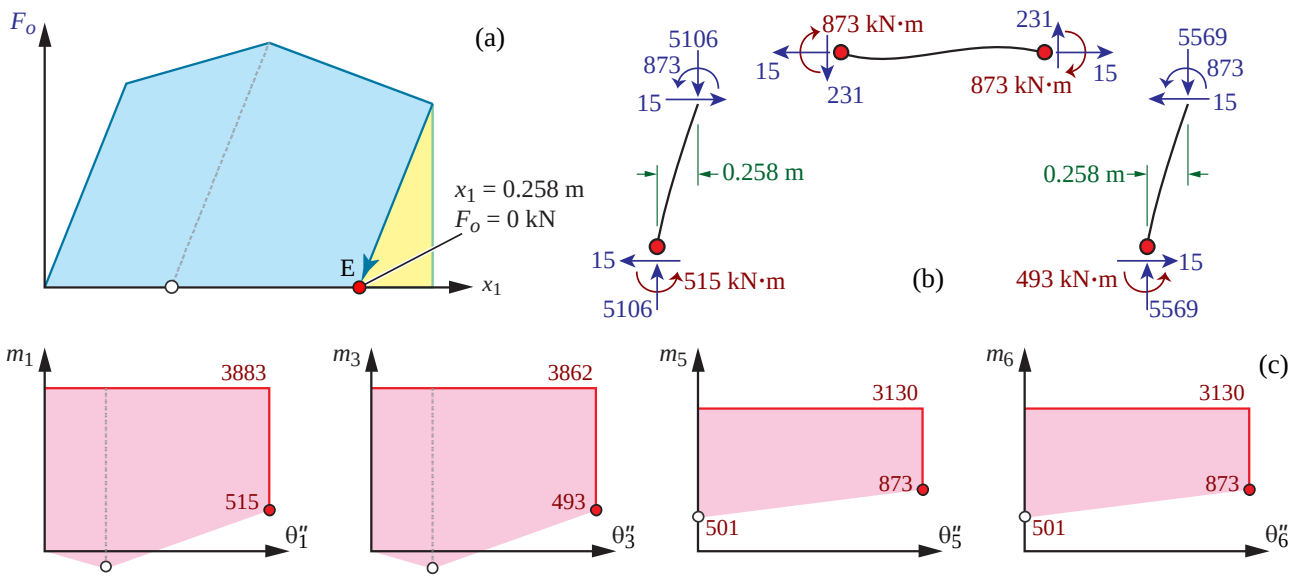

Fig. 6 – State of structure at Point E

6. Numerical Simulation of a 4-story Moment-Resisting Frame

To demonstrate the balance of energy in dynamic analysis, consider the four-story moment-resisting frame as shown in Fig.7a designed according to code [8]. This frame contains 36 DOFs (i.e., $n = 36$), of which 4 are horizontal translations, 16 are vertical translations, and 16 are joint rotations. Also, this frame has a total of 56 PHLs (i.e., $m = 56$). Assume each floor has a mass of 95 000 kg, and gravity load of 431 kN is applied on each exterior column member and 632 kN is applied on each interior column member as shown in Fig.7b. Based on these gravity load on the frame, the stiffness matrices $\mathbf{K}$, $\mathbf{K}'$, and $\mathbf{K}''$ in Eq. (4) are constructed such that geometric nonlinearity is included in the formulation. In addition, a leaning column is used to account for all the gravity loads from other parts of the structure. Let the gravity loads on the leaning column be 3026 kN per floor. Finally, a 2 % damping is assumed in all four modes of vibration.

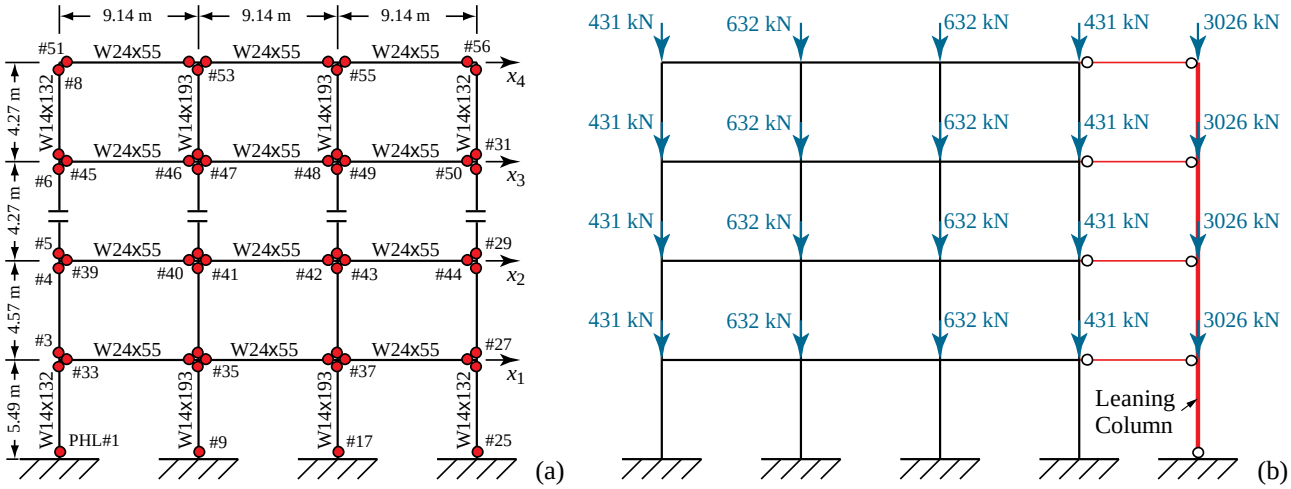

Fig. 7 – Four-story moment-resisting steel frame and corresponding gravity loads

Assume the yield stress of the member is 345 MPa and all 56 plastic hinges exhibit elastic-perfectly-plastic behavior. By subjecting the frame to the 1995 Kobe earthquake ground acceleration shown in Fig.8, the energy response histories are summarized in Fig.9. The results confirm that *KE* and *SE* are always positive (see Fig.9a), *DE* and *PE* are cumulative (see Fig.9b), and *HE* is always negative (see Fig.9d). Of particular interest is Fig.9c, which shows the plot of *IE* and *PE*. This figure shows that significant portion of input energy is dissipated through plastic energy, indicating that significant damage occurs in the structure.

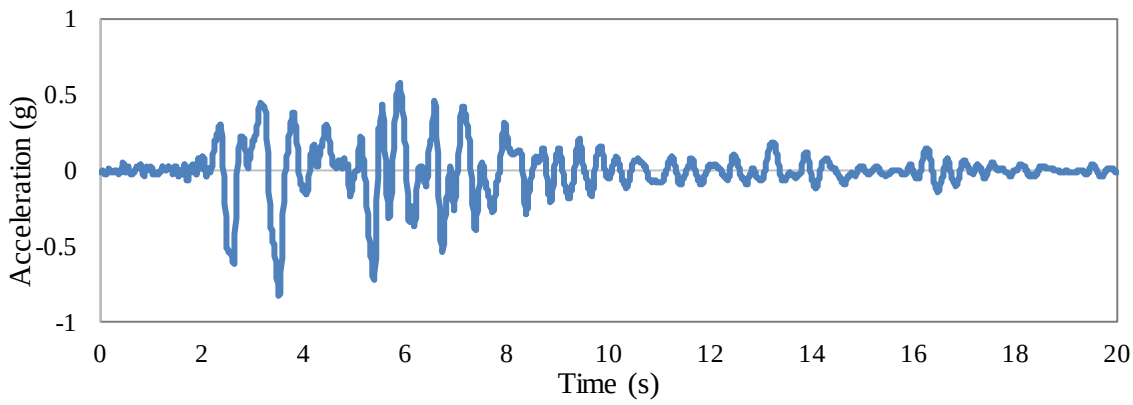

Fig. 8 – Recorded 1995 Kobe earthquake ground motion at Kajima station Component 000

In terms of plastic energy dissipation at individual plastic hinges, Fig.10a shows the maximum plastic energy at each plastic hinge, i.e., PE_i . Since plastic energy accumulates over time, the maximum plastic energy always occurs at the end of the earthquake duration. In addition, summing the plastic energy at all the plastic hinges in Fig.10a gives 950 kJ, which is equal to the total plastic energy dissipation *PE* at the end of the earthquake shown in Fig.9c.

Now consider the same 4-story frame as shown in Fig.7 but is subjected to the Kobe earthquake shown in Fig.8 with a scale factor of 1.4. The energy response histories are shown in Fig.11, where Fig.11a shows the storing energy quantities including *KE*, *SE*, and *HE*, while Fig.11b shows the cumulative energy quantities including *DE*, *PE*, and *IE*. Comparison of results in Fig.11 with those in Fig.9 shows that both *PE* and *IE* increase due to a larger earthquake while other energy quantities remain practically the same. This is consistent with intuition that larger input energy due to larger earthquake must be dissipated through plastic energy, resulting in more structural damage. The plastic energy dissipated in each plastic hinge, i.e., PE_i , is shown in Fig.10b. Summing these individual plastic energy values in Fig.10b gives 1484 kJ, which is equal to the total plastic energy dissipation *PE* at the end of the earthquake shown in Fig.11b.

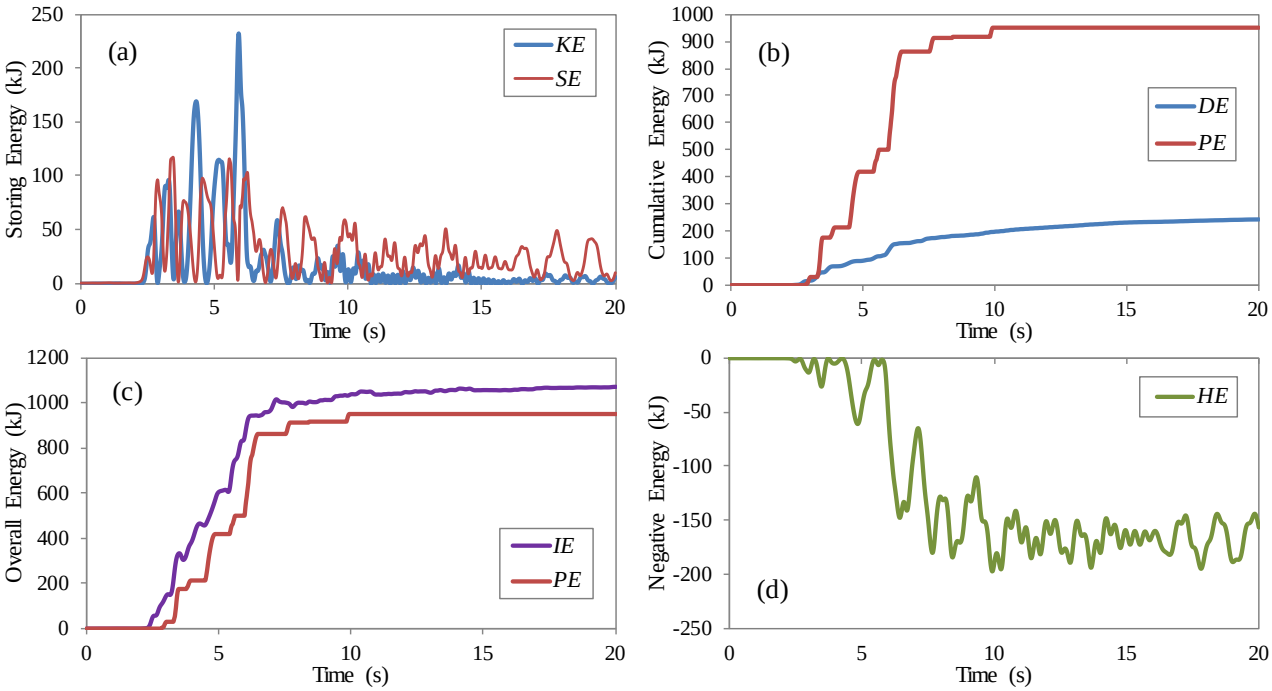

Fig. 9 – Energy responses of the 4-story framed structure due to Kobe earthquake

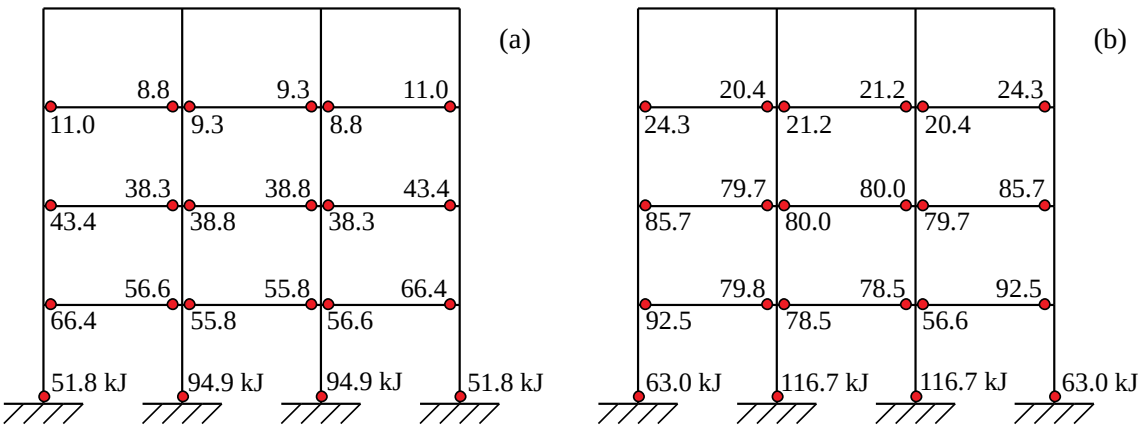

Fig. 10 –Plastic energy dissipation among individual plastic hinges

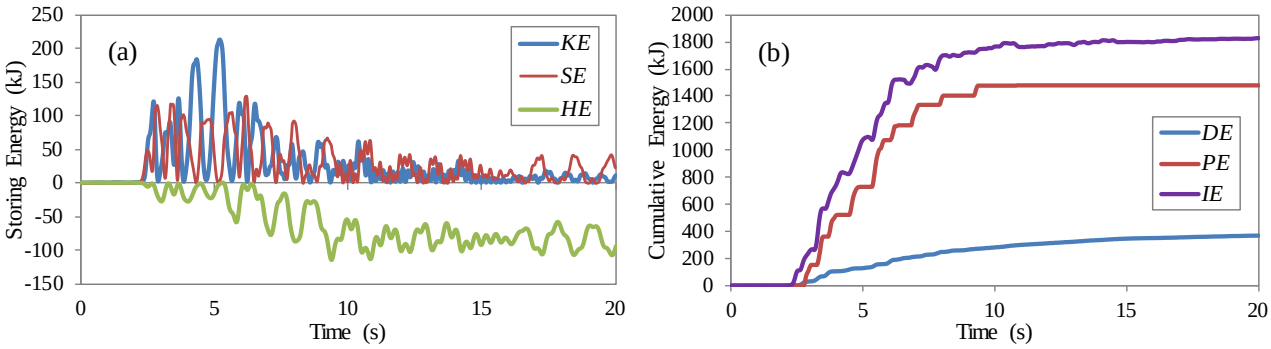

Fig. 11 – Energy responses of the 4-story framed structure due to 1.4 × Kobe earthquake

7. Conclusion

The analytical theory of seismic energy balance and the associated computational method for evaluating the seismic energy in structures are presented with the inclusion of geometric nonlinearity and material nonlinearity. This method successfully separates the coupling effect of material nonlinearity and geometric nonlinearity by using inelastic displacement. By expressing the input energy as the sum of kinetic energy, damping energy, strain energy, higher-order energy, and plastic energy, the energy representation of the structural response due to earthquake ground motion is complete. In particular, the two nonlinear energies are: (1) Higher-order energy (*HE*), which represents the negative energy stored in the structure that can be detrimental to structural stability; and (2) Plastic energy (*PE*), which represents the dissipation of energy and reduction of structural response due to material nonlinearity.

Due to static loading, the summation of these energy forms is exactly equal to the input energy. This is verified step by step in the present paper. The key is that plastic energy requires to use of elastic moment in the calculation, which is contrary to many past research [9-13] that uses total moment to calculate the area underneath the moment-rotation plots. The study is then extended to dynamic analysis, where plastic energy dissipation among individual plastic hinges is calculated. By using the elastic moment in the calculation of plastic energy, it is shown that energy is balanced in a dynamic system. This balance of energy is important because it gives a higher level of confidence in quantifying the energy demand in each component (i.e., PE_i), which in turn can be compared with the energy capacity of each component in energy-based design.

8. References

[1] Tembulkar J, Nau JM (1987): Inelastic modeling and seismic energy dissipation. *Journal of Structural Engineering ASCE*, **113** (6), 1373-1377.

[2] Fajfar P, Vidic T, Fischinger M (1989): Seismic demand in medium-period and long-period structures. *Earthquake Engineering and Structural Dynamics*, **18** (8), 1133-1144.

[3] Fajfar P (1992): Equivalent ductility factors, taking into account low-cycle fatigue. *Earthquake Engineering and Structural Dynamics*, **21** (10), 837-848.

[4] Chai YH (2005): Incorporating low-cycle fatigue model into duration-dependent inelastic design spectra. *Earthquake Engineering and Structural Dynamics*, **34** (1), 83-96.

[5] Uang CM, Bertero VV (1990): Evaluation of seismic energy in structures. *Earthquake Engineering and Structural Dynamics*, **19** (1), 77-90.

[6] Wong KKF, Yang R (2002): Earthquake response and energy evaluation of inelastic structures. *Journal of Engineering Mechanics ASCE*, **128** (3), 308-317.

[7] Wong KKF, Yang R (1999): Inelastic dynamic response of structures using force analogy method. *Journal of Engineering Mechanics ASCE*, **125** (10), 1190-1199.

[8] Harris JL, Speicher MS (2015): *Assessment of First Generation Performance-Based Seismic Design Methods for New Steel Buildings Volume 1: Special Moment Frames*, National Institute of Standards and Technology, USA.

[9] Park YJ, Ang AHS (1985): Mechanistic seismic damage model for reinforced concrete. *Journal of Structural Engineering ASCE*, **111** (4), 722-739.

[10] McCabe SL, Hall WJ (1989): Assessment of seismic structural damage. *Journal of Structural Engineering ASCE*, **115** (9), 2166-2183.

[11] Chai YH, Fajfar P (2000): A procedure for estimating input energy spectra for seismic design. *Journal of Earthquake Engineering*, **4** (4), 539-561.

[12] Bojorquez E, Reyes-Salazar A, Teran-Gilmore A, Ruiz SE (2010): Energy-based damage index for steel structures. *Steel and Composite Structures*, **10** (4), 331-348.

[13] Benavent-Climent A (2011): An energy-based method for seismic retrofit of existing frames using hysteretic dampers. *Soil Dynamics and Earthquake Engineering*, **31** (10), 1385-1396.